Scientia Horticulturae 170 (2014) 228–236

Contents lists available at ScienceDirect

Scientia Horticulturae

journal homepage: www.elsevier.com/locate/scihorti

Effects of grapevine leafroll associated virus 3 infection on growth, leaf gas exchange, yield and basic fruit chemistry of *Vitis vinifera* L. cv. Cabernet Franc

Solomon T. Endeshaw[a,b], Paolo Sabbatini[a,*], Gianfranco Romanazzi[b], Annemiek C. Schilder[c], Davide Neri[b]

[a] Department of Horticulture, Michigan State University, Plant and Soil Sciences Bldg, East Lansing, MI 48824-1325, USA
[b] Department of Agricultural, Food and Environmental Science, Polytechnic University of Marche, Ancona, Italy
[c] Department of Plant, Soil and Microbial Sciences, Michigan State University, East Lansing, MI, USA

ARTICLE INFO

Article history:
Received 12 November 2013
Received in revised form 4 March 2014
Accepted 11 March 2014
Available online 30 March 2014

Keywords:
Vitis vinifera L.
Photosynthesis
Virus
Growth
Fruit quality

ABSTRACT

Grapevine leafroll impacts both vine health and fruit quality and is then one of the most important viral diseases of grapevine (*Vitis vinifera* L.). It occurs in all major grape-growing areas worldwide, and is caused by several grapevine leafroll-associated viruses (GLRaVs). Within causal agents, GLRaV-3 is the predominant strain. Cabernet Franc vines grown at the SWMREC in Benton Harbor, Michigan, USA were grouped as healthy or symptomatic during the spring of 2012, based on symptoms recorded during the previous season. Using enzyme-linked immunosorbent assay, GLRaV-3 was detected only in symptomatic vines, and no others GLRaVs were found. Leaf gas exchange, chlorophyll *a* fluorescence, leaf pigment content and midday relative water content were measured during the growing season. At harvest, yield components and basic fruit chemical parameters were measured. Shoot growth was measured during the growing season. Number of leaves per shoot, shoot leaf area and internode length were measured after the appearance of symptoms. Pruning weight and cane lignification were recorded after the first fall frost. GLRaV-3 infection considerably decreased leaf net photosynthesis, stomatal conductance and transpiration before and after the appearance of symptoms. The effects of GLRaV-3 infection on quantum efficiency of PS II and pigment content were only evident after the development of symptoms, but did not significantly affect midday relative water content. GLRaV-3 inhibited maximum carboxylation efficiency, rate of photosynthetic electron transport, and triose phosphate use by 30%. Yield and soluble solid content per vine were reduced by 40% and 43%, respectively. No significant differences were recorded in phenolic and anthocyanin contents of berries. GLRaV-3 infection significantly reduced number of shoot per vine, shoot growth, shoot leaf area and internode length. The reduction of leaf metabolism induced by GLRaV-3 infection, also decreased vine growth and size and cane lignification. The result showed, GLRaV-3 infection induced a significant reduction in CO_2 assimilation, yield, vine size and cane lignification of cv. Cabernet Franc grown in cool-climate viticultural region.

1. Introduction

Grapevine leafroll occurs in all major grape-growing areas worldwide and is one of the most common and damaging viral diseases of vines (Pearson and Goheen, 1988; Martelli and Boudon-Padieu, 2006). At least ten serologically distinct viruses are associated with leafroll disease (Fuchs, 2007). Grapevine leafroll associated viruses (GLRaVs) represent, except GLRaV-2, a complex of viruses in the genus *Ampelovirus*, family *Closteroviridae* (Martelli et al., 2002), and GLRaV-3 is the predominant viral strain in the world (Engelbrecht and Kasdorf, 1990; Habili et al., 1995; Martin et al., 2005). GLRaV-2 is also associated with leafroll

Abbreviations: DM, dry mass; ELISA, enzyme-linked immunosorbent assay; FM, fresh mass; GLRaVs, grapevine leafroll-associated viruses; HG, healthy grapevines; *J*, rate of photosynthesis electron transport; mRWC, midday relative water content; PSI, photosystem I; PSII, photosystem II; Rubisco, ribulose 1,5-bisphosphate carboxylase/oxygenase; SG, symptomatic grapevines; SWMREC, Southwest Michigan Research and Extension Center; TM, turgid mass; TPU, triose phosphate use; V_{cmax}, maximum carboxylation allowed by rubisco.

* Corresponding author. Tel.: +1 517 355 5191; fax: +1 517 353 0890.
E-mail address: sabbatin@msu.edu (P. Sabbatini).

http://dx.doi.org/10.1016/j.scienta.2014.03.021
0304-4238/

disease but belongs to another genus, *Closterovirus*, within the same family (Fauquet et al., 2005). In Michigan vineyards, grapevine leafroll symptoms are common, and GLRaV-3 is the predominant virus, with GLRaV-1 and GLRaV-2 occurring more rarely (Schilder, 2011). Most grapevine viruses are recognized on the basis of leaf symptoms, depending on effects on chloroplast structure and functioning (Balachandran et al., 1997). Virus biotic stress is poorly understood because inoculation studies are difficult and physiological responses highly variable (Balachandran et al., 1997). Viral diseases in grapevine tend to induce leaf morpho-physiological changes that impact fruit quality (Martelli, 1993; Guidoni et al., 1997). Infected vines generally show inter-venal leaf chlorosis (in white cvs) or reddening (in red cvs) and downward leaf rolling. Those changes are correlated with reduced CO_2 assimilation, stomatal conductance, chloroplast number and chlorophyll metabolism (Hunter and Peat, 1973; Almási et al., 1996). Symptoms generally appear in the summer and in early fall (Hoefort and Gifford, 1967; Weber et al., 1993). Infection with GLRaVs impacts vine growth, yield, berry weight, and sugar and anthocyanin accumulation in the berries and wines. Leafroll disease can cause yield losses of as much as 40% in grapevines (Pearson and Goheen, 1988; Credi and Babini, 1997). Photosynthesis and transpiration are key physiological processes in plants and sensitive to biotic and abiotic stress (Balachandran et al., 1997). Hristov and Abrasheva (2001) using Cabernet Sauvignon measured low levels of chlorophyll and carotenoid pigments in the leaves of GLRaV-3 infected vines compared to healthy vines. Sampol et al. (2003) reported declines in net assimilation rate, stomatal conductance, chlorophyll pigments and non-photochemical quenching in vines infected by both grapevine fanleaf virus and GLRaV-1, -2 and -3. However, most of those studies were performed with vines grown *in vitro* or in pot trials. Under field conditions, other factors such as vine age, cultivar and rootstock interactions as well as training and pruning systems may influence the grapevine physiological response to virus infection (Woodham et al., 1983; Mannini et al., 1996; Credi and Babini, 1997; Guidoni et al., 1997; Sampol et al., 2003).

The aim of this study was to describe the effects of GLRaV-3 infection on leaf physiological parameters (net photosynthesis, chlorophyll *a* fluorescence, chlorophyll content, stomatal conductance, transpiration, and intercellular CO_2 concentration), before and after the appearance of leaf symptoms, and its impact on growth and fruit yield and quality and cane maturation of Cabernet Franc vines grown in Michigan, a cool-climate viticultural region.

2. Materials and methods

2.1. Vineyard site

The experiment was conducted in 2012 at the Southwest Michigan Research and Extension Center (SWMREC) of Michigan State University in Benton Harbor (N 40.09, W 86.36), Michigan, USA. Michigan's climate is characterized by a short growing season (145–175 days) with cool-climate summer conditions (1300 ± 300 growing degree days or GDD, calculated beginning April 1st to October 31st with base 10 °C). Cabernet Franc vines (clone FPS 01) grafted on rootstock 3309C were planted in 1993 in a Spinks sandy loam soil (USDA, 1957) with a spacing of 2.5 m within the row and 3.0 m between rows, with rows oriented N–S. Vines were cane pruned during the winter of 2011 to forty-eight nodes per vine, and trained to vertical shoot positioning (VSP) with a fruit-bearing wire at 1.2 m from the ground and three sets of catch wires at 40-cm intervals from the fruit-bearing wire. During the previous 2 years and the 2012 growing season, no irrigation or fertilizers were applied to the experimental plot. Soil analysis was performed in the spring and showed sufficient levels of macro- and micronutrients (Wise et al., 2008). Recommended crop protection practices were followed and the pest management program was based on scouting, experience and weather conditions. A combination of fungicides and insecticides was used for disease and insect control and chemical classes were alternated to avoid resistance development in target pests and pathogens. Pertinent temperature and rainfall data were recorded during the experiment by an automated weather station from the Michigan Automated Weather Network (MAWN) located on site at 120 m from the experimental vineyard.

2.2. Treatments and experimental design

During 2010, the MSU Viticulture team scouted the Cabernet Franc vineyard at SWMREC and found a high incidence of leafroll. Based on visual observations in 2010 and 2011, and ELISA test carried in the previous seasons for all GLRaVs detectable by ELISA, two groups of four vines were selected as healthy (HG) and symptomatic (SG) in June 2012, before any symptoms were visually present on the leaves. In HG (control) and SG [infected by grapevine leafroll associated virus 3 (GLRaV-3)], two shoots were selected in June 22, 2012 and on each shoot three leaves (basal, middle and apical) were tagged. To reduce the experimental error and environmental variability, eight vines in the same row were selected and two shoots per vine were selected with a completely randomized experimental design.

2.3. Enzyme linked immunosorbent assay (ELISA) diagnosis and symptom development

Leaves and petioles from HG and SG were sampled in June (at bloom) and in the first week of September (3 weeks after veraison). The samples were tested by ELISA for the presence of the following viruses: GLRaV-1, GLRaV-2, GLRaV-3, GLRaV-4-9 [representing five virus strains in a combined kit]), Grapevine fleck virus (GFkV), Grapevine virus A (GVA), Grapevine virus B (GVB), Arabis mosaic virus (ArMV), Grapevine fanleaf virus (GFLV), Tobacco ringspot virus (TRSV), Tomato ringspot virus (ToRSV), and Peach rosette mosaic virus (PRMV) (Clark and Adams, 1977; Zimmermann et al., 1990). Commercial ELISA kits were used for the analyses (Bioreba Ag., Reinach., Switzerland, and Agdia, Inc., Elkhart, IN, USA). The tissue/extraction buffer ratio was 1:20 (w/v Bioreba kits) and 1:10 (w/v Agdia kits). Absorbance at 405 nm was measured using an EL800 Universal Microplate Reader (Bio-Tek Instruments, Winooski, VT).

The degree of symptom development in the canopy was recorded every 10–15 days by counting the number of infected leaves on selected shoots of SG. Then, the degree of symptom development in the canopy was calculated by a simple proportional formula, i.e., percent symptom development = (number of symptomatic leaves per shoot/total number of leaves per shoot) × 100. Additionally, at the end of the season, the prevalence of GLRaV-3 infection in Cabernet Franc vineyard was rated by assessing the percentage of the canopy with leafroll symptoms as healthy (=0%), mild (1–39%), moderate (40–74%) or severe (75–100%).

2.4. Gas exchange, chlorophyll a fluorescence, chlorophyll content and midday relative water content

Gas exchange, chlorophyll *a* fluorescence, and chlorophyll content were determined on selected leaves from July to September, 2012. Midday relative water content (mRWC) was measured on non-selected symptomatic and healthy leaves of selected HG and SG once per month. Net photosynthesis (P_n), stomatal conductance (g_s), transpiration (E) and intercellular CO_2 concentration (C_i) were determined simultaneously on leaves using a CIRAS2 portable

photosynthesis system (PP system, Amesbery, Massachusetts, USA). This PP system was equipped with a leaf-clamped cuvette covering 2.25 cm^2 of leaf area, and measurements were taken under field conditions (i.e. photosynthetically active radiation was $\geq$1500 $\mu mol\ m^{-2}\ s^{-1}$, inlet relative humidity was fixed around 26.7%, and chamber temperature ranged from 26 to 31 °C). The measurements were carried out once every 10–15 days between 10:00 a.m. and 1:00 p.m. (solar time). A week after the first appearance of symptoms on the leaves, the CO_2 response curve was measured on three HG and SG by CIRAS2 using external CO_2. Maximum carboxylation rate allowed by ribulose 1,5-bisphosphate carboxylase/oxygenase (Rubisco) (V_{cmax}), rate of photosynthetic electron transport (J), triose phosphate use (TPU), day respiration (R_d) and mesophyll conductance (R_d) were determined from the A/C_i fitting curve (Sharkey et al., 2007). Chlorophyll *a* fluorescence was quantified on leaves using a Handy PEA chlorophyll fluorometer (Hansatec Instrument, United Kingdom). The initial fluorescence yield (F_o), the variable fluorescence (F_v), and the maximum fluorescence yield (F_m) were assessed in leaves that were dark-adapted for 20 min. The maximum PSII efficiency was calculated according to the methods described by Maxwell and Johnson (2000) and Jifon and Syvertsen (2003), where PSII quantum yield = F_v/F_m for a dark-adapted leaf. For each leaf, the values of the selected fluorescence parameters were averaged. Chlorophyll *a* fluorescence measurements were carried out sequentially on the same leaves, once every 10–15 days. Relative chlorophyll concentrations were estimated using a SPAD-502 chlorophyll meter (Minolta, Tokyo, Japan). Chlorophyll readings (expressed as SPAD units) were taken repeatedly at the three apices of a triangle drawn on the leaf lamina, once every 10–15 days on selected leaves of HG and SG.

The midday relative water content (mRWC) was determined from detached leaf portions (about 1 cm^2). Four leaves per treatment were sampled at midday and stored in a polyethylene plastic bag. The leaf portions were cut and weighed immediately to obtain the fresh mass (FM). They were then placed overnight in the dark in a beaker (25 cm^3) filled with deionized water. They were reweighed the next morning to obtain the turgid fresh mass (TM), while the dry mass (DM) was recorded after drying the leaf portions at 80 °C for 24 h in an oven. The mRWC of the leaves was calculated as $mRWC = [(FM - DM)/(TM - DM)] \times 100\%$.

2.5. Yield components and basic fruit chemistry

Fruit yield per vine was measured at harvest (end of September) and the number of clusters per vine was counted. From each tagged shoot, clusters were separately collected and weighed. The number of berries, and mean cluster and berry weight per vine were then determined. Furthermore, both cluster length and the number of seeds per berry were determined by measuring the rachis length and counting seeds after dissecting the berry, respectively. The chemical composition of the fruit was analyzed for each vine using a 20-count berry sample collected on the day of harvest and frozen for later analysis (Iland et al., 2004). Prior to analysis, berries were thawed at 24 °C for 12 h. Grape juice soluble solids (°Brix) were analyzed using an Atago refractometer (Atago USA, Inc, Kirkland, Washington, USA), and the pH was measured using a 370 Thermo Orion (Beverly, Massachusetts, USA) pH meter. An automatic titrator, coupled to an autosampler and control unit (Titroline 96, Schott, Germany) was used to determine titratable acidity. Additionally, sugar content per vine was determined by multiplying sugar content per berry by yield according to Poni et al. (2008). Total anthocyanins and phenolics were determined on the 20-count berry sample per vine as described by Iland et al. (2004). Berries were homogenized at high speed (24,000 rpm) using a Brinkmann homogenizer (Brinkmann Instruments, Westbury, New York, USA) for about 1 min. Approximately, 1 ± 0.05 g of homogenized sample was added to a pre-tared 15-mL centrifuge tube, enriched with 10 mL (50%, v/v) aqueous ethanol acidified to pH 2. The sample with aqueous ethanol was mixed for 1 h, by shaking on a vortex-geniemixer (Scientific Industries, Bohemia, New York, USA) once every five to ten minutes, before centrifugation (20 min at 5000 rpm). One mL of the extract (supernatant liquid) was added to 10 mL 1 M HCL and equilibrated for 3 h, and the absorbance values were registered with a UV–vis spectrophotometer (Model UV-1800, Shimadzu Corporation, Kyoto, Japan) at 280, 520 and 700 nm. Total anthocyanin content was expressed as mg per g of fresh berry weight and phenolics as absorbance units (a.u.) per g of fresh berry weight.

2.6. Shoot growth, vine size, and cane lignification

Seasonal shoot growth was tracked and recorded for both HG and SG vines. Four shoots per vine were selected and tagged in June and shoot growth was measured every 15–30 days until September 12. For each selected shoot, the number of internodes was recorded in late August, and mean internode length was determined by dividing shoot length by the number of internodes. In addition, 1 week after the first appearance of symptoms, ten shoots from each unselected HG and SG were sampled, stored in a polyethylene plastic bag and transported to the laboratory. The number of leaves per shoot, shoot length, and leaf area per shoot were determined by counting, measuring with tape (meter) and using an Li-3100 Area Meter (Li. COR, Inc. Lincoln, Nebraska, USA), respectively. After the first fall frost, HG and SG vines were pruned and the pruning weight per vine recorded and used as an index of vine size and for the calculation of the Ravaz Index (RI) (Ravaz, 1911). Canes of HG and SG vines were taken to the laboratory, and cane lignification was visually rated for the first five internodes as lignified (dark brown), mildly lignified (brown) or not lignified (light green) as reported by Sabbatini et al. (2012).

2.7. Statistical analysis

Basic statistics, including analysis of variance, regression and correlation analysis were performed using the STATISTICA software package (Statsoft, Tulsa, Oklahoma, USA) and Sigma Plot (version 10; SPSS, Chicago, IL, USA). Data were tested for normality and homogeneity of variance prior to being subjected to the *F*-test, and differences were considered significant when $p < 0.05$ and highly significant when $p < 0.01$.

3. Results

3.1. Weather data

Weekly average weather data (rainfall, maximum and minimum temperature) at the SWMREC experimental site for the study period from July to September, 2012 are shown in Fig. 1. During this period, the hottest and driest period occurred from mid-June to mid-August. After mid-August, precipitation increased and both the maximum and minimum temperatures started to decrease considerably by early September, levelling off in October. The maximum weekly precipitation (48 mm) was recorded in mid-August.

3.2. Yield and basic fruit chemistry

Grapevines infected by GLRaV-3 (SG plants) showed a significant reduction in yield with over 40% loss compared to HG. The yield reduction was mostly a function of the reduction in the number of clusters per vine and berry weight. In fact, the number of clusters

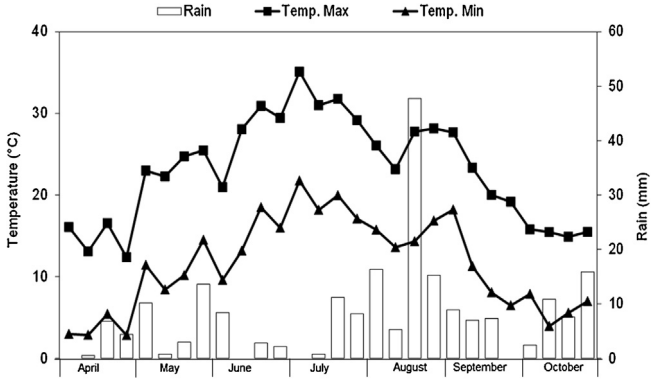

Fig. 1. Weekly mean rainfall and maximum and minimum temperature data at the Southwest Michigan Research and Extension Center (SWMREC) in Benton Harbor (Michigan, USA) from April to October 2012.

Table 1
Yield parameters of healthy (HG) and GLRaV-3-infected (SG) Cabernet Franc grapevines in Benton Harbor, Michigan, USA in 2012.

Parameter[x]	HG	SG
Yield (kg/vine)	7.4 ± 0.5a	4.8 ± 0.4b
Cluster/vine (*n*)	76 ± 7.1a	55 ± 3.2b
Cluster length (cm)	17 ± 0.9a	15 ± 1.8a
Cluster weight (g)	97.5 ± 6.8a	82.7 ± 4.3a
Berries/cluster (*n*)	71.2 ± 5.1a	67.2 ± 3.4a
Berry weight (g)	1.36 ± 0.0a	1.23 ± 0.0b
Berry dry weight (%)	27.8 ± 0.8a	23.7 ± 1.0b
Berry diameter (mm)	12.4 ± 0.1a	12.2 ± 0.1a
Seed/berry (*n*)	2.5 ± 0.2a	2.3 ± 0.2a

[x] Values are means ± SE ($n = 4$). Means in a row followed by the same letter are not significantly different at $p = 0.05$.

per vine, berry weight, berry diameter, and berry dry matter content were all significantly reduced by GLRaV-3 infection. Cluster length, cluster weight, the number of berries per cluster, and the number of seeds per berry also were reduced in SG compared to HG but the differences were not statistically significant (Table 1). Basic fruit chemistry was also affected by GLRaV-3 infection, both during berry development (data not shown) and at harvest (Table 2). At harvest, a lower total soluble solids content per vine was recorded in SG ($947 \pm 96\,g\,l^{-1}$ vine^{-1}), 43% lower than HG. Differences were also observed in soluble solids (°Brix) and TA in SG compared to HG, in vines having the same balance as indicated by the RI. The decrease in pH was minimal in SG. GLRaV-3 infection did not significantly reduce the phenolic and anthocyanin content of berries in SG compared to HG (Table 2).

3.3. Shoot growth, pruning weight and cane lignification

GLRaV-3 infection had a negative impact on the number of shoots, shoot length, pruning weight, and cane lignification (Table 3, Fig. 2). In SG, the number of shoots was significantly

Table 2
Composition of juice collected from healthy (HG) and GLRaV-3-infected (SG) Cabernet Franc grapevines in Benton Harbor, Michigan, USA in 2012.

Parameter[a]	HG	SG
Brix (°Bx)	22.4 ± 0.27a	20.7 ± 0.22b
pH	3.47 ± 0.04a	3.43 ± 0.01a
Titratable acidity ($g\,l^{-1}$)	6.1 ± 0.34°	7.3 ± 0.35a
Sugar per vine ($g\,l^{-1}$ vine^{-1})	1657 ± 106a	925 ± 90b
Anthocyanin ($mg\,g^{-1}$)	0.76 ± 0.03a	0.75 ± 0.04a
Phenolic ($a.u.\,g^{-1}$)	1.11 ± 0.10a	1.10 ± 0.12a

[a] Values are means ± SE ($n = 4$). Means in a row followed by the same letter are not significantly different at $p = 0.05$.

Table 3
Growth parameters of healthy (HG) and GLRaV-3-infected (SG) Cabernet Franc grapevines in Benton Harbor, Michigan, USA in 2012.

Parameter[x]	HG	SG
Shoot per vine (*n*)	40.2 ± 2.0a	27.7 ± 4.6b
Clusters per shoot (*n*)	1.9 ± 0.2a	2.0 ± 0.3a
Internode length (cm)	5.1 ± 0.1a	4.5 ± 0.3a
Pruning weight (kg)	2.9 ± 0.5a	1.8 ± 0.3b
Ravaz Index (RI)[y]	2.6 ± 0.2a	2.7 ± 0.3a
Cane lignification (index)[z]	2.57 ± 0.1a	2.01 ± 0.2b

[x] Values are means ± SE ($n = 4$). Means in a row followed by the same letter are not significantly different at $p = 0.05$.

[y] Ravax index is the ratio between yield (kg) and pruning weight (kg) per vine (Ravaz, 1911).

[z] Cane lignification (index) is a number from 1 to 3 given for the internode to characterize cane maturation based on the color (dark brown-3, brown-2 or light green-1) (Sabbatini et al., 2012).

reduced by 31%, as compared to HG. Shoot growth in SG stopped at the end of June, but in HG shoot growth continued until the end of July (Fig. 2). It was evident that GLRaV-3 infection significantly reduced pruning weight, by 38%, and lignification of the canes, which resulted in a mildly lignified condition in SG and highly lignified in HG (Table 3).

3.4. ELISA diagnosis and symptom development

Among the tested viruses, only GLRaV-3 was found in the SG (data not shown). No viruses were detected in healthy plants. During the experiment, visual leaf symptoms and the impact on vine phenology were recorded on vines infected by GLRaV-3. At bloom, symptomatic grapevines (SG) showed reduced vine growth (Fig. 2) and a 7-day delay in fruit-set, consequently delaying the time of veraison. The typical symptoms of an infected leaf, interveinal reddening and downward leaf rolling, appeared in mid-August and developed, with higher severity on basal leaves, on the selected shoots and continued to develop towards the shoot apex affecting up to 80% of the vine leaf area at harvest (Fig. 3). GLRaV-3 infection also reduced internode length and increased leaf formation but with reduced leaf area (Fig. 4). At the end of the 2012 growing season, visual observation of the spatial distribution showed a high prevalence of leafroll infection in the Cabernet Franc vineyard with about 76% of the vines showing typical symptoms. Among the infected vines, 40%, 29% and 31% showed severe, moderate and mild symptoms, respectively. At the end of September, all the SG showed a severe infection while HG remained asymptomatic (Fig. 5).

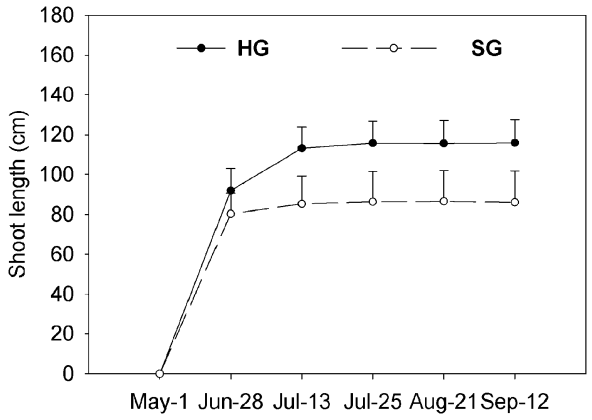

Fig. 2. Shoot growth during the season (from May to September, 2012) in healthy (HG) and GLRaV-3-infected (SG) Cabernet Franc grapevines in Benton Harbor, Michigan, USA. Data are mean ± SE ($n = 4$).

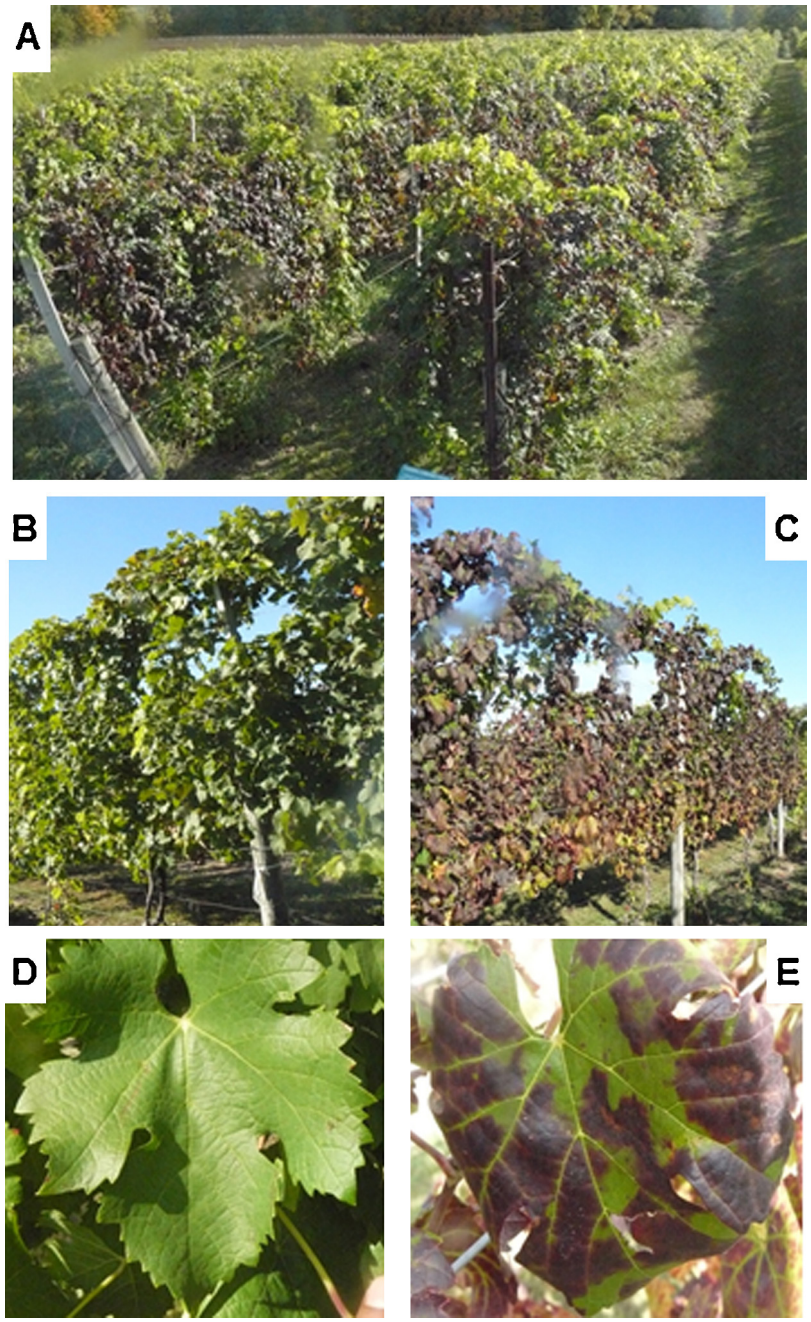

Fig. 3. Bird's eye view of Cabernet Franc plot in Benton Harbor, Michigan, USA in 2012 (A), healthy grapevines (HG) with no visual symptoms in the canopy (B), symptomatic grapevines (SG) with visual appearance of leafroll symptoms in the canopy (C), healthy/control leaf of HG with normal appearance (D) and symptomatic leaf of SG with rolling of margins and interveinal reddening (E).

3.5. Gas exchange

In HG leaves, net photosynthesis (P_n) was relatively stable at 13.8 μmol m^{-2} s^{-1} over the season, from July to September. All SG showed a highly-significant reduction in P_n, before and after the development of visual GLRaV-3 symptoms on the leaves, by 27–70% of the HG levels in the period from July to September (Fig. 6A). In HG leaves, stomatal conductance (g_s) was higher and remained stable around 630 mmol m^{-2} s^{-1} with a minimal decrease in August. In the SG leaves g_s was significantly reduced even before visual appearance of the symptoms on the leaves in July, by 28% as compared to the HG leaves. The reduction of g_s on SG leaves was further exacerbated after the appearance of the foliar symptoms and decreased further during the growing season, reaching the lowest level (67% as compared to HG leaves) in September (Fig. 6B). Contrary to P_n and g_s, which remained stable during the season in HG leaves, transpiration (E) in HG leaves decreased up to 21% when compared to HG leaves in July. The E differences between SG and HG leaves were highly significant before the appearance of visual symptoms, increased after appearance of visual symptoms and development along the shoot, and then reached a maximum reduction, about 40%, in September in SG leaves as compared to HG leaves (Fig. 6C). In HG leaves, internal CO_2 concentration (C_i) remained stable throughout the season but increased during the season in SG leaves commensurate with the development of visual symptoms (Fig. 6D). The HG and SG showed distinctly different P_n patterns along the shoot during the season. In SG, P_n continuously increased along the shoot and attained a maximum at the

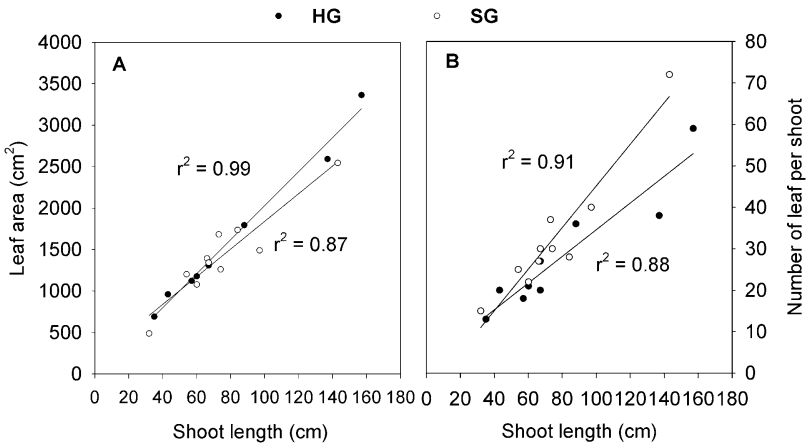

Fig. 4. Correlation between shoot length to leaf area per shoot (A) and number of leaves per shoot (B) of healthy (HG) and GLRaV-3-infected (SG) Cabernet Franc grapevines in Benton Harbor, Michigan, USA in 2012.

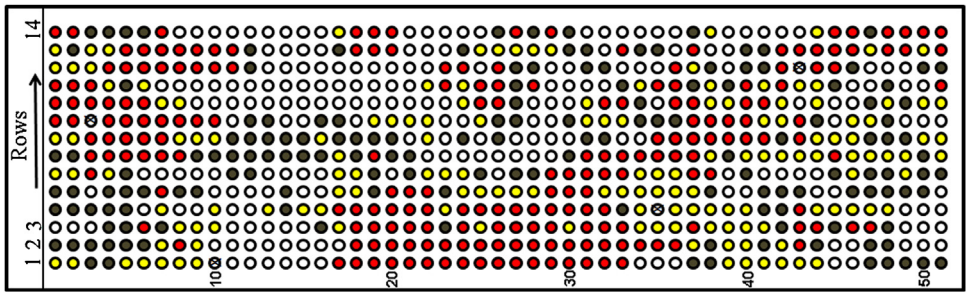

Fig. 5. Spatial distribution of grapevine leafroll symptoms (GLRaV-3) in a Cabernet Franc vineyard at SWMREC in Benton Harbor, Michigan, USA at the end of September, 2012. Each circle represents a vine. Healthy vines (those that did not show foliar symptoms) are marked in white. Infected vines (those that showed symptoms) are marked in red (severe: ≥75% of the foliage symptomatic), yellow (moderate: 40–74% of the foliage symptomatic) and grey (mild: <40% of the foliage symptomatic). X represents a missing vine. For this experiment, vines from 12 to 15 and from 19 to 22 in the second row were used as healthy and symptomatic vines respectively.

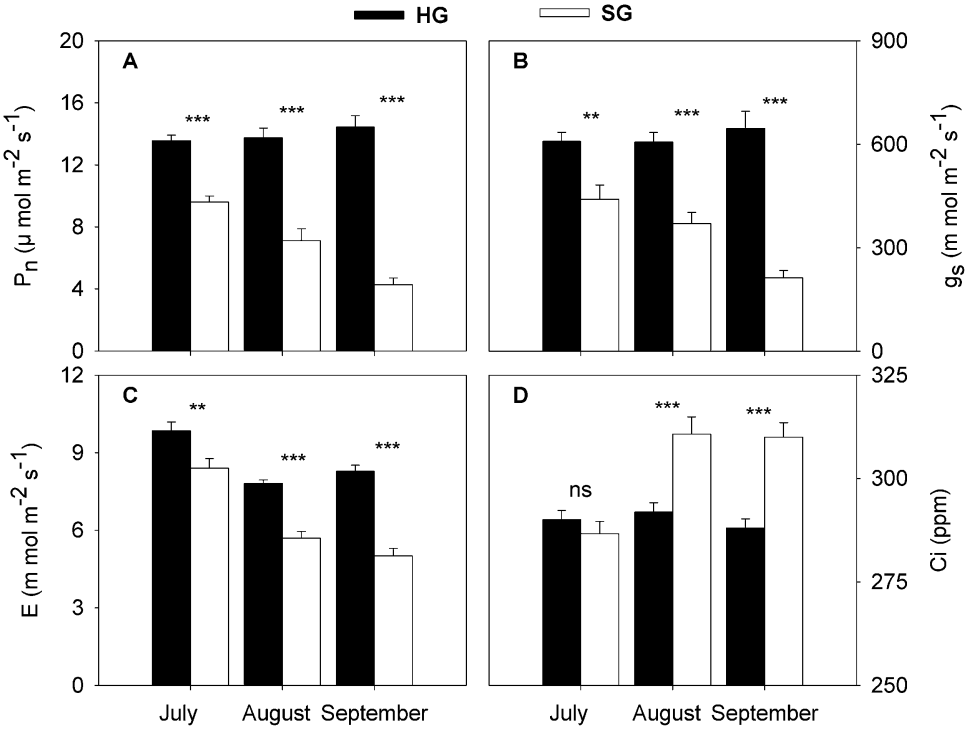

Fig. 6. Change in photosynthetic parameters over the season from July to September, 2012 in foliage of healthy (HG) and GLRaV-3-infected (SG) Cabernet Franc grapevines in Benton Harbor, Michigan, USA: (A) net photosynthesis (P_n), (B) stomatal conductance (g_s), (C) transpiration (E), (D) intercellular CO_2 (C_i). Data are mean + SE ($n = 4$). Means in the same month marked with *, ** and *** are significantly different at $p < 0.05$, $p < 0.01$ and $p < 0.001$ respectively, whereas ns indicates no statistical difference (F test).

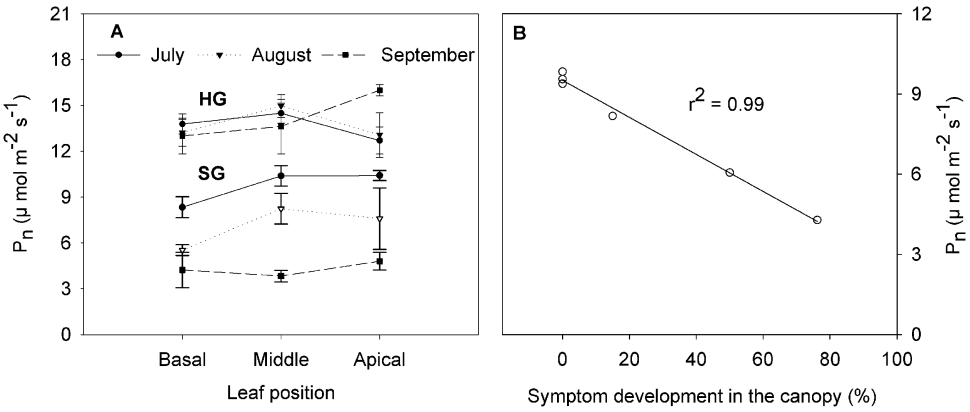

Fig. 7. (A) Change in net photosynthesis (P_n) along the shoot from July to September, in healthy (HG) and GLRaV-3-infected (SG) Cabernet Franc grapevines in Benton Harbor, Michigan, USA: and (B) correlation between GLRaV-3 symptom development and net photosynthesis. Data are mean ± SE (n = 4).

apex throughout the growing season. In HG, P_n increased along the shoot and attained a maximum in the middle of the shoot in July and August and at the apex of the shoot in September (Fig. 7A). Similarly, the correlation between P_n and symptom development (r^2 = 0.99) in SG during the growing season showed a direct relation between decreasing leaf assimilation rate and symptom development (Fig. 7B). The A/C_i response curve, 1 week following the appearance of symptoms, in SG leaves demonstrated a significant reduction in maximum carboxylation efficiency (V_{cmax}), rate of photosynthetic electron transport (J), triose phosphate use (TPU), and day respiration (R_d) (Table 4).

3.6. Chlorophyll a fluorescence, chlorophyll content and midday relative water content

Before the appearance of symptoms in July, the maximum quantum efficiency of PSII (F_v/F_m) in HG and SG leaves was similar (0.77 and 0.78, respectively). But after the appearance of the symptoms in SG leaves, in August and until harvest, the F_v/F_m values were significantly reduced. The decrease in this F_v/F_m ratio in SG leaves was mainly due to an increase in F_o (about 19%, data not shown) compared to the HG leaves. In the HG leaves, the F_v/F_m was similar throughout the study period (around 0.76) (Fig. 8A).

GLRaV-3 infection did not affect chlorophyll content of the leaf before the appearance of symptoms, but after the appearance of symptoms a significant reduction in total chlorophyll content was observed. In HG leaves, total chlorophyll content increased during the season and reached 41 ± 0.6 SPAD units in September. Total chlorophyll content in SG leaves decreased by 21% and 26% in August and September, respectively, when compared with HG leaves (Fig. 8B).

In both HG and SG leaves, midday relative water content (mRWC) was decreased during the season as compared to the being of the season. The decrease in mRWC in infected leaves was higher than in HG leaves, but this reduction was not significant (Fig. 8C).

Table 4
A/C_i curve parameters of healthy (HG) and GLRaV-3-infected (SG) Cabernet Franc grapevines in Benton Harbor, Michigan, USA in 2012.

Parameter[x]	HG	SG
V_{cmax} (m mol m^{-2} s^{-1})	286.9 ± 18	201.5 ± 18
J (m mol m^{-2} s^{-1})	1211.8 ± 68	835.8 ± 74
TPU (m mol m^{-2} s^{-1})	102.6 ± 5	71.0 ± 6
R_d (m mol m^{-2} s^{-1})	282.8 ± 18	199.3 ± 18
g_m (m mol m^{-2} s^{-1} Pa^{-1})	11.5 ± 0.1	10.8 ± 0.5

Where: V_{cmax}, maximum carboxylation allowed by rubisco; J, rate of photosynthesis electron transport; TPU, triose phosphate use; R_d, day respiration; and g_m, mesophyll conductance.

[x] Values are mean ± SE (n = 3).

4. Discussion

Our ELISA analysis of symptomatic grapevines (SG) performed in June and September confirmed the detection of GLRaV-3 in the leaves. The net photosynthesis (P_n), stomatal conductance (g_s), and transpiration (E) were significantly reduced when compared to healthy grapevines (HG) throughout the study period, before and after the visual appearance of the symptoms on the leaves (Fig. 6). A similar result was also reported in Chardonnay infected with Bois noir phytoplasma (Endeshaw et al., 2012). In our trials, in SG leaves, even before the development of the symptoms, the changes due to GLRaV-3 infection were not localised in the basal portion of the shoot, where symptoms first appeared, but P_n was significantly reduced in the middle and apical portion of the shoot as well. This was further confirmed by the reduction in the maximum carboxylation efficiency allowed by rubisco (V_{cmax}) and the rate of photosynthetic electron transport (J) in SG (Table 4). Similar effects were also been reported by Moutinho-Pereira et al. (2012) on Touriga Nacional infected by GLRaV-1 and -3 and by Endeshaw et al. (2012) on Chardonnay infected by Bois noir phytoplasma that was healthy in the previous year and showed symptoms in the middle of the season. In contrast, in HG leaves, basal, middle and apical, P_n, g_s and E did not show significant differences through the season and maintained high values. In addition, the similar in midday relative water content between HG and SG leaves before and after visual appearance of the symptom on the leaf, when leaf water potential drops to the minimum, indicated that stomatal closure in SG was independent of whole vine water stress, but it might marks the multiplication of GLRaV-3 in the phloem vessels. Moreover, stomatal limitation does not appear to be the main factor that lead to reduction in P_n. In SG leave, after visual appearance of the symptom, in parallel to the decrease in P_n and stomatal conductance, C_i was significantly higher. This indicate that CO_2 fixation was limited by internal process within SG leaves, and it is likely that the decrease in g_s was an indirect consequence.

A SPAD meter determines the greenness (density of color) and the interaction of thylakoid chlorophyll with light incident (Jifon et al., 2005), while the chlorophyll a fluorescence, expressed as F_v/F_m, reflects the leaf photosynthesis intensity as it arises from the absorbed light energy that is not used for photosynthetic reactions and heat dissipation (Oxborough, 2004). The HG leaves showed efficient PS II activity (F_v/F_m) and increasing leaf pigment content during the season. GLRaV-3 infected vines showed a significant decrease in F_v/F_m ratio and leaf pigment content after visual

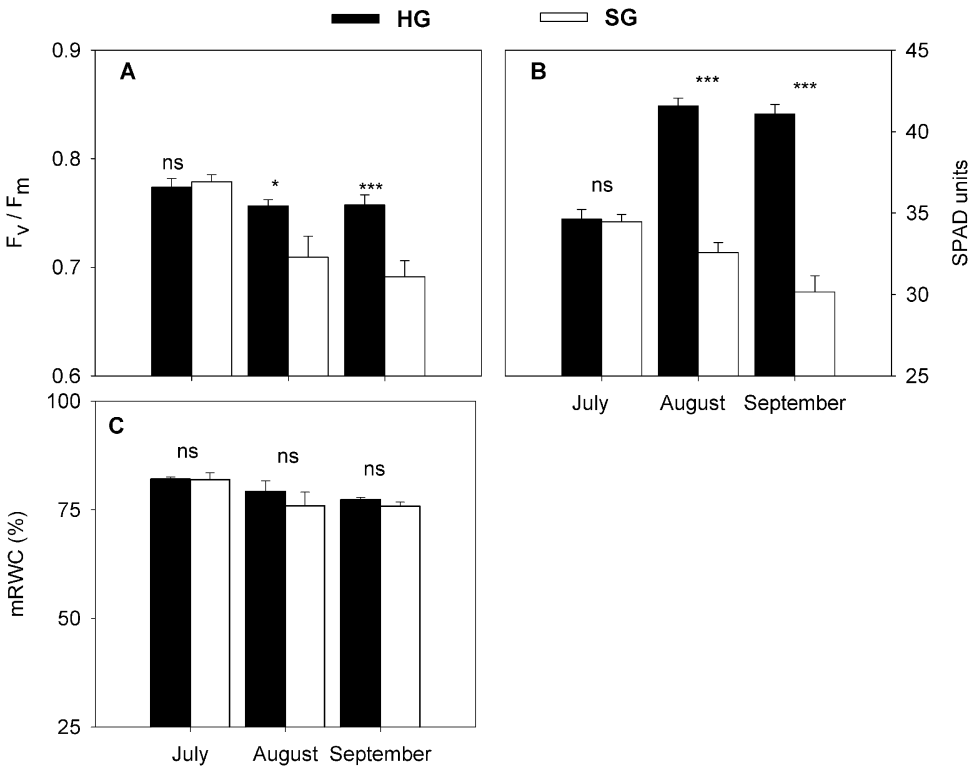

Fig. 8. Change in various physiological parameters over the season from July to September, 2012 in healthy (HG) and GLRaV-3-infected (SG) Cabernet Franc grapevines in Benton Harbor, Michigan, USA: (A) maximum quantum efficiency (F_v/F_m), (B) total chlorophyll content (chl a + b) and (C) midday relative water content (mRWC). Data are mean ± SE ($n = 4$). Means in the same month marked with *, ** and *** are significantly different at $p < 0.05$, $p < 0.01$ and $p < 0.001$, respectively, whereas ns indicates no statistical difference (F test).

appearance of the symptoms and similar values to that of HG leaves before development of symptoms on the leaf (Fig. 8). The decrease in maximum quantum efficiency of PSII in SG leaves was due to decreased variable fluorescence (F_v) without decreasing the F_m level. This is characteristic of the inhibition of the accepter side of PSII (Allakhverdiev et al., 1987; Setlik et al., 1990). The similar total chlorophyll content in HG and SG leaves, before the appearance of symptoms and the consequent increase in HG and small decrease in SG, indicate that GLRaV-3 impairs leaf maturation and chloroplast development by enlarge other than chloroplast degradation.

The reduction in grapevine metabolism of Cabernet Franc, induced by GLRaV-3 infection, had a direct influence on berry size, clusters per vine, vine size, and cane lignification of SG (Tables 1 and 3; Figs. 2 and 4). Indeed, infected vines suffered a drastic yield decrease of about 40%. Similar effects of GLRaV infection on Chardonnay production have been found in other studies carried out in north-eastern Italy and in Sardinia with grapevines affected by Bois noir phytoplasma (Garau et al., 2007). We also recorded perturbations in the qualitative parameters of the grape juice (brix, vine soluble solids content, TA), which indicated modifications in the carbon allocation and partitioning in the vine (Table 2). Similar consequences have been observed for vines affected by phloematic microrganisms, like Bois noir phytoplasma, or viruses GVA, GLRaV-1, and GLRaV-3, the elimination of which results in increased yield, improved grape quality parameters and sensory characteristics of the resulting wines (Komar et al., 2007; Endeshaw et al., 2012). GVA, GLRaV-1 and Rupestris stem pitting associated virus (GRSPaV) infection in Nebbiolo influenced protein synthesis involved in response to oxidative stress in the berry skin and cell structure metabolism of the pulp (Giribaldi et al., 2011). Our results confirm that Cabernet Franc is highly susceptible to leafroll as is evident from percentage of symptomatic vines in the experimental vineyard (Figs. 3 and 5). The virus was likely introduced with the planting material. The spatial pattern observed does suggest that spread may have occurred over insects (e.g., mealybug) over time. Alternatively, the severity of symptom expression could be related to variability in stresses, such as imposed cultural treatments, soil variability or nutrition. From our results, it appears that gas exchange, vine growth, yield components and fruit chemistry makeup at harvest can detect differences between healthy and infected vines. In fact, symptomatic leaves showed a dramatic decrease in P_n and g_s values, and the reduced sugar accumulation (per berry and per vine) can be explained by the progressive loss of leaf functionality during the growing season caused by the GLRaV-3. Also, our observations suggest that, when the disease does not cause symptoms on vines, early in the season (from bloom to veraison), the leaf photosynthetic performance and associated metabolic components (chlorophyll, nitrogen content) of the infected grapevines was most probably undermined.

In conclusion, the mechanisms of GLRaV-3 development still have to be further elucidated, and experimental studies combining viticultural and pathological components are promising to understand how this virus affects vine physiology, fruit quality and most importantly the survival of grapevines in cool-climate viticultural regions. These results can help growers understand the negative consequences of GLRaV-3 infection on their vines and aid in deciding on vine replacement. They also stress the importance of using certified propagating materials when establishing a new vineyard.

Acknowledgments

This research was supported by AgBioResearch at Michigan State University (Project GREEEN) and the Southwest Michigan Research and Extension Center as part of the cooperative agreement between Michigan State University (Department of

Horticulture) and Polytechnic University of Marche (Department of Agricultural, Food and Environmental Science). This research was in partial fulfillment of requirements for the Doctoral Degree of S. Endeshaw. We thank P. Murad, D. Acimovic, S. Zhuang, L. Tozzini and A. Green for assistance with collecting data, D. Francis for help with vineyard maintenance, J. Gillett for ELISA tests of grape samples, and A. Green for critical reading of the manuscript.

References

Allakhverdiev, S.I., Setlikova, E., Klimov, V.V., Setlik, I., 1987. In photoinhibited photosystem II particles pheophytin in photoreduction remains unimpaired. Febs. Lett. 226, 186–190.

Almási, A., Eke', M., Gaborjaínyi, R., 1996. Comparison of ultrastructural changes of *Nicotiana benthamiana* infected with three different viruses. Acta. Phytopathol. Entomol. Hung. 31, 181–190.

Balachandran, S., Hurry, V.M., Kelley, S.E., Osmond, C.B., Robinson, S.A., Rohozinski, J., Seaton, G.G., Sims, D.A., 1997. Concepts of plant biotic stress, some insights into stress physiology of virus-infected plants, from the perspective of photosynthesis. Physiol. Plant. 100, 203–213.

Clark, M.F., Adams, A.N., 1977. Characteristics of the microplate method of ELISA for the detection of plant viruses. J. Gen. Virol. 34, 475–483.

Credi, R., Babini, A.R., 1997. Effects of virus and virus-like infections on growth, yield and fruit quality of Albana and Trebbiano Romagnolo grapevines. Am. J. Enol. Viticult. 48, 7–12.

Endeshaw, S.T., Murolo, S., Romanazzi, G., Neri, D., 2012. Effects of Bois noir on carbon assimilation, transpiration, stomatal conductance of leaves and yield of grapevine (*Vitis vinifera*) cv Chardonnay. Physiol. Plant. 145, 286–295.

Engelbrecht, D.J., Kasdorf, G.G.F., 1990. Field spread of corky bark, fleck, leafroll and Shiraz decline diseases and associated viruses in South African grapevines. Phytophylactica 22, 347–354.

Fauquet, C.M., Mayo, M.A., Maniloff, J., Desselberger, U., Ball, L.A., 2005. Virus Taxonomy: VIIIth Report of the International Committee on Taxonomy of Viruses. Elsevier Academic.

Fuchs, M.F., 2007. Grape Leafroll Disease. Cornell University, www.nysipm.cornell.edu/factsheets/grapes/diseases/grape_leafroll.pdf

Garau, R., Sechi, A., Prota, V.A., Moro, G., 2007. Productive parameters in Chardonnay and Vermentino grapevines infected with "Bois noir" and recovered in Sardinia. Bull. Insectol. 60, 233–234.

Giribaldi, M., Purrotti, M., Pacifico, D., Santini, D., Mannini, F., Caciagli, P., Rolle, L., Cavallarin, L., Giuffrida, M.G., Marzachì, C., 2011. A multidisciplinary study on the effects of phloem-limited viruses on the agronomical performance and berry quality of *Vitis vinifera* cv Nebbiolo. J. Proteomics 75, 306–315.

Guidoni, S., Mannini, F., Ferrandino, A., Argamante, N., Di Stefano, R., 1997. The effect of grapevine leafroll and rugose wood sanitation on agronomic performance and berry and leaf phenolic content of a Nebbiolo clone (*Vitis vinifera* L.). Am. J. Enol. Viticult. 48, 438–442.

Habili, N., Fazeli, C.F., Ewart, A., Hamilton, R., Cirami, R., Saldarelli, P., Minafra, A., Rezaian, M.A., 1995. Natural spread and molecular analysis of grapevine leafroll-associated virus 3 in Australia. Phytopathology 85, 1418–1422.

Hoefort, L.L., Gifford, E.M., 1967. Grapevine leafroll virus. History and anatomical effects. Hilgardia 38, 403–426.

Hristov, I., Abrasheva, P., 2001. Effect of grapevine fanleaf virus and grapevine leafroll associated virus 3 on vine plants under conditions of *in vitro* cultivation. Rastenievudni Nauki 38, 269–274.

Hunter, C.S., Peat, W.E., 1973. The effect of tomato aspermy virus on photosynthesis in the young tomato plant. Physiol. Plant Pathol. 3, 517–527.

Iland, P., Bruer, N., Edwards, G., Weeks, S., Wilkes, E., 2004. Chemical Analysis of Grapes and Wine; Techniques and Concepts. Patrick Iland Wine Promotions Pty Ltd., Adelaide, Australia, pp. p110.

Jifon, J.L., Syvertsen, J.P., 2003. Moderate shade can increase net gas exchange and reduce photoinhibition in citrus leaves. Tree Physiol. 23, 119–127.

Jifon, J.L., Syvertsen, J.P., Whaley, E., 2005. Growth environment and leaf anatomy affect nondestructive estimates of chlorophyll and nitrogen in Citrus sp. leaves. J. Am. Soc. Hortic. Sci. 130, 152–158.

Komar, V., Vigne, E., Demangeat, G., Fuchs, M., 2007. Beneficial effect of selective virus elimination on the performance of *Vitis vinifera* cv Chardonnay. Am. J. Enol. Viticult. 58, 202–210.

Mannini, F., Argamante, N., Credi, R., 1996. Improvements in the quality of grapevine Nebbiolo clones obtained by sanitation. Acta Hortic. 427, 319–324.

Martelli, G.P., 1993. Graft-transmissible diseases of grapevines. In: Handbook for Detection and Diagnosis. FAO Publication Division, Rome.

Martelli, G.P., Agranovsky, A.A., Bar-Joseph, M., Boscia, D., Candresse, T., Coutts, R.H.A., Dolja, V.V., Falk, B.W., Gonsalves, D., Jelkmann, W., Karasev, A.V., Minafra, A., Namba, S., Vetten, H.J., Wisler, G.C., Yoshikawa, N., 2002. The family *Closteroviridae* revised. Arch. Virol. 147, 2039–2044.

Martelli, G.P., Boudon-Padieu, E., 2006. Directory of Infectious Diseases of Grapevines and Viroses and Virus-like Diseases of the Grapevine: Bibliographic Report 1998–2004 , Bari, Italy.

Martin, R.R., Eastwell, K.C., Wagner, A., Lamprecht, S., Tzanetakis, I.E., 2005. Survey for viruses of grapevine in Oregon and Washington. Plant Dis. 89, 763–766.

Maxwell, K., Johnson, G.N., 2000. Chlorophyll fluorescence—a practical guide. J. Exp. Bot. 51, 659–668.

Moutinho-Pereira, J., Correia, C.M., Gonçalves, B., Bacelar, E.A., Coutinho, J.F., Ferreira, H.F., Lousada, J.L., Cortez, M.I., 2012. Impacts of leafroll-associated viruses (GLRaV-1 and -3) on the physiology of the Portuguese grapevine cultivar 'Touriga Nacional' growing under field conditions. Ann. Appl. Biol. 160, 237–249.

Oxborough, K., 2004. Imaging of chlorophyll *a* fluorescence: theoretical and practical aspects of an emerging technique for the monitoring of photosynthetic performance. J. Exp. Bot. 55, 1195–1205.

Pearson, R.C., Goheen, A.C., 1988. Compendium of Grape Diseases. The American Phytopathological Society, St. Paul, MN.

Poni, S., Bernizzoni, F., Civardi, S., 2008. The effect of early leaf removal on whole-canopy gas exchange and vine performance of *Vitis vinifera* L 'Sangiovese'. Vitis 47, 1–6.

Ravaz, M.L., 1911. L'effeullage de la vigne. Annales de L'Ecole Nationale d'Agriculture de Montpellier 11, 216–244.

Sabbatini, P., Howell, G.S., Striegler, K., Wolpert, J., Tozzini, L., 2012. Assessing grapevine cold hardiness status using cane morphology indicators. Italus Hortus 3, 171–175.

Sampol, B., Bota, J., Riera, D., Medrano, H., Flexas, J., 2003. Analysis of the virus-induced inhibition of photosynthesis in malmsey grapevines. New Phytol. 160, 403–412.

Schilder, A., 2011. Diagnosis of grapevine virus disease in Michigan vineyard. In: Research report to Michigan Grape and Wine Industry Council, https://www.michiganwines.com/docs/Research/11schilder2.pdf

Setlik, I., Allakhverdiev, S.I., Nedbal, L., Setlikova, E., Klimov, V.V., 1990. Three types of photosystem II photoinactivation. Photosynth. Res. 23, 39–48.

Sharkey, T.D., Bernacchi, C.J., Farquhar, G.D., Singsaas, E.L., 2007. Fitting photosynthetic carbon dioxide response curves for C_3 leaves. Plant Cell Environ. 30, 1035–1040.

U.S. Department of Agriculture, 1957. Soil Conservation Service, major soils of the north central region, U.S.A. Map. In: Soil Survey North Central Regional Publication 76. Government Printing Office, Washington.

Weber, E., Golino, D., Rowhani, A., 1993. Leafroll disease of grapevines. Practical Winery Vineyard 13, 21–25.

Wise, J.C., Gut, L.J., Isaacs, R., Schilder, A.M.C., Sundin, G.W., Zandstra, B., Beaudry, R., Lang, G., 2008. Michigan Fruit Management Guide. Bulletin E-154, Michigan State University Extension [E-154].

Woodham, R.C., Krake, L.R., Cellier, K.M., 1983. The effect of grapevine leafroll plus yellow speckle disease on annual growth, yield and quality of grapes from Cabernet Franc under two pruning systems. Vitis 22, 324–330.

Zimmermann, D., Bass, P., Legin, R., Walter, B., 1990. Characterization and serological detection of four closterolike particles associated with leafroll disease on grapevine. J. Phytopathol. 130, 205–218.